

# Scattering of low-energy antiprotons by nuclei

O. D. Dal'karov and V. A. Karmanov

*Lebedev Physics Institute, Academy of Sciences of the USSR*

(Submitted 21 May 1985)

*Zh. Eksp. Teor. Fiz.* **89**, 1122–1133 (October 1985)

We show that the mechanism for the interaction of low-energy antiprotons ( $\bar{p}$ ) with nuclei is given by the Glauber model with allowance for Coulomb scattering. We calculated the differential cross sections for  $\bar{p}^{12}\text{C}$  elastic and inelastic scattering (with excitation of the  $2^+$  (4.44 MeV) level of the residual nucleus) as well as for  $\bar{p}^{40}\text{Ca}$  and  $\bar{p}^{208}\text{Pb}$  elastic scattering at incident-particle energies of 46.8 and 180 MeV, without using free parameters. The results turn out to be in good agreement with the data from the Low Energy Antiproton Ring (LEAR). We also determined the ratio of the real to the imaginary parts of the elementary  $\bar{p}N$  amplitude at these energies; these results are also in good agreement with the LEAR data on  $\bar{p}p$  scattering.

## 1. INTRODUCTION

Since the low-energy antiproton ring (LEAR) came into operation, the differential cross sections for elastic scattering and inelastic scattering (with excitation of nuclear levels) of antiprotons with energies  $T_{\bar{p}}$  of 46.8 and 180 MeV by  $^{12}\text{C}$  nuclei and for elastic scattering by  $^{40}\text{Ca}$  and  $^{208}\text{Pb}$  have been measured.<sup>1,2</sup> The results of Refs. 1 and 2 show that the differential cross sections (unlike those for proton scattering at the same energies) clearly exhibit diffractive behavior.

The central problem for a theoretical analysis of the antiproton-nucleus cross sections (as for the theory of nuclear reactions in general) is that of the mechanism of the process. Knowledge of the mechanism is doubtless of considerable interest in itself, but it is also necessary in order to extract information on the antinucleon-nucleon interaction and on nuclear structure from the antinucleon-nucleus cross sections.

In this paper we show that the mechanism for scattering of low-energy antiprotons by nuclei is given by the Glauber theory of diffractive scattering,<sup>3</sup> despite the fact that it would seem at first glance that the conditions for the applicability of the Glauber approximation are not satisfied (an energy of 46.8 MeV corresponds to a momentum  $k$  of  $\sim 300$  MeV/c, which is comparable with the momenta of the intranuclear nucleons). Using the Glauber theory of multiple scattering, we calculate the differential cross sections for elastic scattering and inelastic scattering (with excitation of a level of the residual nucleus) of antiprotons by the  $^{12}\text{C}$  nucleus and the cross sections for elastic scattering by  $^{40}\text{Ca}$  and  $^{208}\text{Pb}$ . These results, some of which have already been published<sup>4</sup> in shortened form, turn out to be in very good agreement with the available experimental data. Next, using the Glauber mechanism for antiproton-nucleus scattering, the validity of which has already been established, we show that, as a result, the scattering of antiprotons by nuclei can provide a convenient means for determining the most indeterminate parameter of the  $\bar{p}N$  amplitude, i.e., the ratio

$$\varepsilon = \text{Re } f_N(0) / \text{Im } f_N(0),$$

where  $f_N(0)$  is the amplitude for  $\bar{p}N$  scattering at zero angle.

Our analysis also shows that the effective radius of the nucleus in antinucleon-nucleus interactions appreciably exceeds the size of the nucleus (by a factor of 1.5 in the case of  $^{12}\text{C}$ ).

We note that in Refs. 2, 5, and 6, the antiproton-nuclear cross sections were calculated using an optical potential; in Refs. 2 and 6, the data of Refs. 1 and 2 were used to determine the optical-potential parameters, while in Refs. 5 the optical potential was obtained using a microscopic approach. When the optical potential is calculated microscopically (in our case using the Glauber approximation) both approaches should, in principle, be equivalent (the optical potential corresponding to the Glauber amplitude was calculated for  $^{12}\text{C}$  in Ref. 4). However, the Glauber approach seems to us to be preferable since it leads to the simplest formulas for the  $\bar{p}$ -nucleus amplitudes that are suitable for an analytic analysis and yields the most direct relation between the  $\bar{p}N$  amplitudes and the  $\bar{p}$ -nucleus amplitude.

The scheme of the exposition is as follows: In section 2 we discuss the conditions under which the Glauber approximation is applicable. In section 3 and 4 we derive formulas for the amplitudes for elastic and inelastic scattering of antiprotons by nuclei. In sections 5 and 6 we compare the calculated elastic and inelastic cross sections with the experimental data and show that the mechanism for the scattering of antiprotons by nuclei is indeed the Glauber mechanism. From an analysis of the differential cross sections at the diffraction minima, we show that the scattering of antiprotons by nuclei makes it possible to eliminate the present ambiguity in measuring the quantity  $\text{Re } f_N(0) / \text{Im } f_N(0)$  for the elementary  $\bar{p}N$  amplitude.

## 2. LIMITS OF APPLICABILITY OF THE GLAUBER APPROXIMATION

The following two conditions are necessary for the applicability of the Glauber approach: 1) the eikonal approximation must be valid so that the motion of the incident particle can be regarded as rectilinear, or nearly so; 2) the

motions of the intranuclear nucleons must be adiabatic so that it may be assumed that the positions of the nucleons in the nucleus remain fixed during the flight time of a beam particle through the nucleus (the nucleons are "frozen-in"). Both conditions are simultaneously satisfied at high energies, but, as noted above, they seem to be violated at energies  $T_{\bar{p}}$  of the order of 50 MeV. In the case of antinucleons, however, there is reason to believe that the range of applicability of the Glauber approximation is greatly extended and that the approximation can be used down to very low incident-antinucleon energies.

The point is that the validity of the eikonal approximation may be assured by the sharp forward directivity of  $\bar{p}N$  scattering at low energies, the inclination of the cone increasing with decreasing energy. For comparison, the inclination of the  $\bar{p}p$ -scattering cone at 46.8 MeV is  $35.6 (\text{GeV}/c)^{-2}$  (Ref. 7), while the  $pp$  scattering is virtually isotropic at the energy<sup>8</sup> and the inclination of the  $pp$ -scattering cone does not exceed  $\sim 6(\text{GeV}/c)^{-2}$  even at high energies.

We note that the appearance of such a narrow cone at low energies and its narrowing with decreasing energy are due, in turn, to the fact that even at the lowest energies there is a substantial contribution to  $N\bar{N}$  scattering from several partial waves having non-zero orbital angular momenta. As was shown in Ref. 9, this phenomenon is not associated with annihilation processes, but is due to the presence of a spectrum of quasinuclear  $N\bar{N}$  states corresponding to non-zero orbital angular momenta  $l$  with respect to the motion of the  $N$  and  $\bar{N}$  particles (the levels exist in virtually all spin-isospin states<sup>10</sup>). It is precisely this that leads to the considerable enhancement of the contribution to low-energy  $\bar{p}p$  scattering from partial waves clear up to  $l = 3$ . The total number of partial waves (taking into account the different spin-isospin states) amounts to  $\approx 20$ . The interference between the partial waves leads to the sharp forward directivity of  $\bar{p}N$  scattering at low energies.

As regards the nonadiabatic corrections, we note that, as was shown in Ref. 11, they are compensated to a considerable extent by the departure of the amplitude for the elementary process from the energy shell. However, the treatment of Ref. 11 was limited to the deuteron. We note that the application of the Glauber theory to  $\bar{p}d$  scattering at low and medium energies yielded fairly good results.<sup>12</sup> For heavier nuclei, the results of Ref. 11 together with the arguments given above in favor of the eikonal approximation can serve only as guidelines. In the absence of an exhaustive theoretical study of the true limits of applicability of the Glauber approximation we can judge these limits only by comparing the calculations with the experimental data. In particular, the cross sections at the diffraction minima are very sensible to corrections to the Glauber mechanism. In sections 5 and 6 we show that the data of Refs. 1 and 2 speak in favor of the applicability of the Glauber approximation clear down to antiproton energies of  $\sim 50$  MeV.

### 3. THE ELASTIC SCATTERING AMPLITUDE

The scattering of low-energy antiprotons by nuclei is unique because, while the Glauber approximation is applicable, the Coulomb effects, which substantially affect the cross

sections at the diffraction minima and at small angles, are very important. These Coulomb effects are important even for light nuclei, but not for the scattering of high-energy hadrons. In the Glauber approach, the Coulomb effects are taken into account by adding the Coulomb phase shift<sup>3</sup> to the nuclear scattering phase shift. With allowance for the Coulomb effects, the amplitude for elastic scattering by a nucleus of mass number  $A$  may be expressed as follows<sup>3,13</sup>;

$$e^{i\chi_0} F_{el}(q) = F_c(q) + ik \int_0^\infty J_0(qb) e^{i\chi_0(b)} \times [1 - \exp(i(\chi_N(b) + \chi_l(b)))] b db, \quad (1)$$

where

$$F_c(q) = -2\xi \frac{k}{q^2} \exp(i\varphi_c), \quad (2)$$

$$\varphi_c = -2\xi \ln\left(\frac{q}{2k}\right) + 2\eta, \quad \eta = \arg \Gamma(1+i\xi), \quad (3)$$

$$\chi_0(b) = 2\xi \ln kb, \quad (4)$$

$$\chi_1(b) = 8\pi\xi \int_b^\infty \rho(r) \left\{ \ln \left[ \frac{1 + (1 - b^2/r^2)^{1/2}}{b/r} \right] - (1 - b^2/r^2)^{1/2} \right\} r^2 dr, \quad (5)$$

where  $J_0(q, b)$  is the Bessel function, and the Coulomb phase shift  $\chi_c$  is the sum of  $\chi_0$  and  $\chi_1$ . In Eqs. (2)–(5)  $\xi = -Z\alpha/k$ , where  $Z$  is the nuclear charge and  $\alpha = e^2/\hbar c$ ; the minus sign in the formula for  $\xi$  corresponds to the case of Coulomb attraction. Equation 1 includes the unimportant screening phase shift

$$\chi_s = -2\xi \ln(2kR_s).$$

The nuclear phase shift  $\chi_N$  has the form<sup>3</sup>

$$\chi_N(b) = \frac{A}{2\pi k} \int e^{-i\mathbf{q}\cdot\mathbf{r}} f_N(\mathbf{q}) \Phi(\mathbf{q}) d^3q, \quad (6)$$

where

$$\Phi(\mathbf{q}) = \int \rho(\mathbf{r}) e^{i\mathbf{q}\cdot\mathbf{r}} d^3r, \quad (7)$$

$\mathbf{q}$  is the momentum transferred to the nucleus,  $k$  is the momentum of the incident hadron, and  $\rho(r)$  is the nuclear density (normalized to unity). We assume that the charge density  $\rho(r)$  in Eq. (5) coincides with the nuclear density. The scattering amplitude per nucleon is

$$f_N(q) = \frac{k\sigma(i+\varepsilon)}{4\pi} e^{-1/2 B q^2}. \quad (8)$$

We used the following values for the  $\bar{p}N$ -amplitude parameters<sup>7,14</sup> at  $T_{\bar{p}} = 46.8$  MeV:  $\sigma_{\bar{p}p} = 200$  mb,  $\sigma_{\bar{p}n} = 200$  mb,  $\varepsilon_{\bar{p}p} = \varepsilon_{\bar{p}n} = 0$ , and  $B_{\bar{p}p} = B_{\bar{p}n} = 35.6 (\text{GeV}/c)^{-2} = 1.4$  Fm<sup>2</sup>. We obtained the value of  $\sigma_{\bar{p}n}$  from the quantity<sup>14</sup>  $\sigma_{\bar{p}d} = 380$  mb with allowance for the Glauber correction for screening.<sup>3</sup>

The  $\bar{p}N$ -amplitude parameters for  $T_{\bar{p}} = 180$  MeV are as follows<sup>7,15</sup>:  $\sigma_{\bar{p}p} = 157$  mb,  $\sigma_{\bar{p}n} = 136$  mb,  $\varepsilon_{\bar{p}p} = \varepsilon_{\bar{p}n} = 0.2$ , and  $B_{\bar{p}p} = B_{\bar{p}n} = 22.2 (\text{GeV}/c)^{-2} = 0.86$  Fm<sup>2</sup>.

The nuclear density in the range  $4 \leq A \leq 16$  is parametrized in the form<sup>16</sup>

$$\rho(r) = [A (R\pi^{1/2})^3]^{-1} [4 + 2/3(A-4) (r/R)^2] e^{-r^2/R^2}, \quad (9)$$

where  $R^2 = 2.50$  Fm<sup>2</sup> for <sup>12</sup>C (Ref. 16). With the parametri-

zation (9), the phase shift  $\chi_N(b)$  can be calculated analytically. For heavier nuclei the nuclear density is given by the Woods-Saxon formula:

$$\rho(r) = \frac{\rho_0}{1 + \exp((r-R)/\tau)}, \quad (10)$$

where  $R = r_0 A^{1/3}$ ,  $r_0 = 1.07$  Fm,  $\tau = 0.545$  Fm,<sup>17</sup>  $\rho_0 = 4 \times 10^{-3}$  Fm<sup>-3</sup> for <sup>40</sup>Ca and  $\rho_0 = 0.8732 \times 10^{-3}$  Fm<sup>-3</sup> for <sup>208</sup>Pb.

An analytic calculation of the phase shift  $\chi_N(b)$  using the density (10) is impossible, while a numerical calculation is more cumbersome than in the case of scattering of high-energy hadrons since the amplitude  $f_N(q)$  cannot be taken out from under the integral sign in (6) because of the large value of the parameter  $B$  in (8). We approximated the density (10) by the formula

$$\rho(r) = \sum_{n=1}^{12} c_n e^{-nr^2/r_a^2}, \quad (11)$$

and used the result to calculate the phase shift  $\chi_N(b)$  analytically. The values of the parameters in (11) are as follows:

$$\begin{aligned} r_a &= 3.5 \text{ Fm}, \quad c_1 = 0.213135E-3, \quad c_2 = 0.129343E-1, \\ c_3 &= 0.355696E-1, \quad c_4 = 0.325283E-1, \quad c_5 = c_8 = c_{10} = c_{12} \\ &= -0.509357E+0, \quad c_6 = 0.553112E+0, \quad c_7 = 0.377754E+0, \\ c_9 &= -0.137796E+0, \quad c_{11} = 0.116708E+1. \end{aligned}$$

for <sup>40</sup>Ca, and

$$\begin{aligned} r_a &= 5.5 \text{ Fm}, \quad c_1 = -0.20703125E-3, \quad c_2 = 0.12043945E-1, \\ c_3 &= -0.21903613E+0, \quad c_4 = 0.20959717E+1, \\ c_5 &= -0.83987627E+1, \\ c_6 &= 0.15549395E+2, \quad c_7 = c_8 = c_{10} = -0.98158730E+1, \\ c_9 &= 0.19602791E+2, \quad c_{11} = -0.24616211E+0, \\ c_{12} &= 0.10524658E+1, \end{aligned}$$

for <sup>208</sup>Pb. The relative accuracy of the approximation is of the order of 1% or better for <sup>40</sup>Ca in the interval  $0 < r < 8$  Fm and for <sup>208</sup>Pb in the interval  $0 < r < 10$  Fm.

The recoil of the nucleus was taken into account by multiplying the amplitude by the factor<sup>13</sup>  $\exp(\langle r^2 \rangle q^2 / 6A)$ . For the parametrization (9) we have  $\langle r^2 \rangle = R^2((5/2) - (4/A))$ ; accordingly  $\langle r^2 \rangle = 12.1$  Fm<sup>2</sup> for <sup>40</sup>Ca and  $\langle r^2 \rangle = 28.2$  Fm<sup>2</sup> for <sup>208</sup>Pb. We used the average of the amplitudes for scattering by a proton and by a neutron in place of  $f_N(q)$  in Eq. (6).

We note that the elastic-scattering amplitude without allowance for the Coulomb effects<sup>3</sup> is

$$F_{el}(q) = ik \int_0^\infty \Gamma(b) J_0(qb) b db, \quad (12)$$

where

$$\Gamma(b) = 1 - \exp(i\chi_N(b)). \quad (13)$$

#### 4. THE INELASTIC-SCATTERING AMPLITUDE

In the single-inelastic-collision (SIC) approximation, the amplitude for inelastic scattering with excitation of a nuclear level having the natural parity, angular momentum  $J$ , and component  $M$  along the incident beam may be expressed in terms of the electromagnetic transition form factor and the elastic-scattering amplitude.<sup>18</sup> We take the Coulomb effects in inelastic scattering into account, using the Coulomb phase shift in the elastic-scattering amplitude, which also occurs in the inelastic amplitude. A single event in which a level is excited takes place only as a result of the strong interaction of the incident hadron with an intranuclear nucleon. The expression obtained in Ref. 18 for the inelastic amplitude can be conveniently written, after allowing for the Coulomb scattering, in the form

$$e^{i\chi_0} F_{inel}^M(q) = \int_0^\infty G_{JM}(b) J_M(qb) db, \quad (14)$$

where

$$G_{JM}(b) = c_{JM} A f_N(0) \mathcal{S}_{JM}(b) b \exp(i(\chi_N(b) + \chi_0(b) + \chi_1(b))), \quad (15)$$

the phase shifts  $\chi_0$ ,  $\chi_1$ , and  $\chi_N$  being given by Eqs. (4)–(6),

$$c_{JM} = (-1)^M \frac{2\pi^{1/2}}{(2J+1)^{1/2}} Y_{JM} \left( \frac{\pi}{2}, 0 \right), \quad (16)$$

$$\mathcal{S}_{JM}(b) = \int_0^\infty S_J(q) e^{-i/2 B q^2} J_M(qb) q dq, \quad (17)$$

and  $S_J(q)$  determines the electromagnetic form factor for the inelastic transition and is parametrized in the form

$$S_J(q) = q^J (a_1 + b_1 q^2 + c_1 q^4) e^{-\alpha q^2}, \quad (18)$$

which makes it possible to calculate the integral (17) analytically.<sup>4</sup> The parameters in (18) are known from data on inelastic scattering of electrons. For the excitation of the  $2^+$  (4.44 MeV) level of <sup>12</sup>C we used the following values<sup>19</sup> of the parameters  $a_1 = 0.25$ ,  $b_1 = -0.021$ ,  $c_1 = 0.0004$ , and  $\alpha = 0.54$ , the value of the variable  $q$  in (18) being expressed in reciprocal fermis.

#### 5. COMPARISON WITH EXPERIMENT: ELASTIC SCATTERING

The calculated cross sections presented below are very sensitive to the  $\bar{p}N$ -amplitude parameters (8), and especially to the ratio of the real to the imaginary parts of  $\varepsilon$ . At present the uncertainty in the value of  $\varepsilon$  is very great, while the data from different groups of investigators contradict one another. This is evident from the summary of data<sup>15</sup> shown in Fig. 1. In our calculations we shall use the values of  $\varepsilon$  obtained from LEAR experiments, but for comparison we also present calculations using the value of  $\varepsilon$  from Ref. 20.

In Figs. 2–4 the cross sections for antiproton elastic scattering by <sup>12</sup>C, <sup>40</sup>Ca, and <sup>208</sup>Pb nuclei at energies of 46.8 and 47.8 MeV are presented and compared with the data of Refs. 1 and 2. The solid curves were calculated with allowance for Coulomb scattering at  $\varepsilon = 0$  (the LEAR value,<sup>15</sup> see Fig. 1). The dash-dot curves on Figs. 2–4 show the

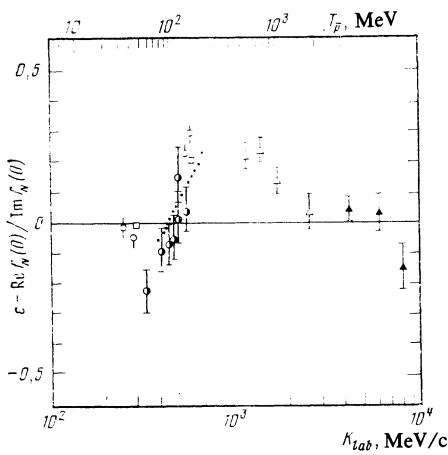


FIG. 1. The ratio  $\varepsilon = \text{Re} f_N(0)/\text{Im} f_N(0)$  for the  $\bar{p}N$  scattering amplitude.  $\circ$ —LEAR data (Ref. 15);  $\bullet$ —from Ref. 20;  $\bullet$ —from Ref. 25;  $\square$ —values of  $\varepsilon$  obtained in the present work from  $\bar{p}$ -nucleus cross sections;  $\triangle$  and  $\blacktriangle$ —from Ref. 20.

Rutherford-scattering cross section for a point charge of strength  $Ze$  [the squared modulus of the amplitude (2)] in order to illustrate the magnitude of the Coulomb scattering. The dotted curve shows the cross section at  $\varepsilon = 0$  without allowance for Coulomb scattering. At the minimum of the cross section on Fig. 2 and at the second minimum on Fig. 3 the dotted curve practically coincides with the dashed curve. The dashed curves show the cross sections for  $\varepsilon = -0.25$  (Ref. 20). The filling of the diffraction minima for  $\varepsilon = 0$  and their considerable deepening for  $\varepsilon = -0.25$  is due to the Coulomb-nuclear interference, the cross sections being very sensitive to the value of  $\varepsilon$  (except in the case of  $^{208}\text{Pb}$ , where the predominant part played by the Coulomb effects weakens the sensitivity of the cross section to  $\varepsilon$ ). The great sensitivity of the cross section to  $\varepsilon$  is due to the fact that in the absence of Coulomb scattering the magnitude of the cross section at the diffraction minima is proportional to  $\varepsilon^2$  (Ref. 4).<sup>1)</sup> In the presence of Coulomb-nuclear interference, the

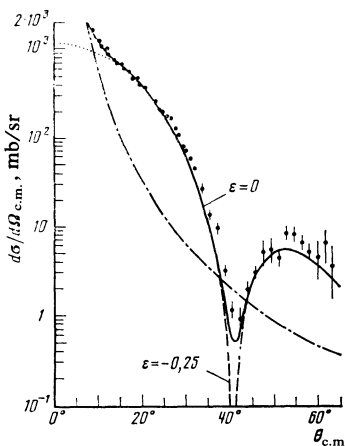


FIG. 2. The differential cross section for  $\bar{p}^{12}\text{C}$  elastic scattering at 46.8 MeV. The full curve is for  $\varepsilon = 0$ ; the dashed curve is for  $\varepsilon = -0.25$ ; the dotted curve is for purely nuclear scattering; the dash-dot curve is for Coulomb scattering by a point charge  $Z$ .

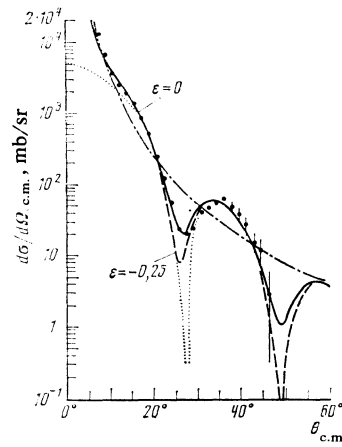


FIG. 3. Differential cross section for  $\bar{p}^{40}\text{Ca}$  elastic scattering at 46.8 MeV. The notation is the same as in Fig. 2.

dependence of the cross section at the minima on  $\varepsilon$  becomes more complicated, but, as before, it remains very high, the cross section becoming sensitive to the sign of  $\varepsilon$  (this was noted before in Ref. 13).

Thus, a good description of the cross sections for scattering by  $^{12}\text{C}$ ,  $^{40}\text{Ca}$ , and  $^{208}\text{Pb}$  nuclei at 46.8 MeV is obtained for the value  $\varepsilon = 0$ . The value  $\varepsilon = -0.25$  is excluded by experimental data<sup>1,2</sup> on antiproton scattering by nuclei.

On the other hand, it is significant that scattering of protons of the same energy by  $^{12}\text{C}$  does not reveal any considerable diffractive behavior,<sup>1</sup> while Glauber-model calculations of the  $p^{12}\text{C}$  cross section do not agree with experiment (see Ref. 4).

Figures 5–7 show the cross sections for elastic scattering of antiprotons by  $^{12}\text{C}$ ,  $^{40}\text{Ca}$ , and  $^{208}\text{Pb}$  nuclei at energies of 179.7 and 180.3 MeV, together with data from Refs. 1 and 2 for comparison. The cross sections are still very sensitive to the value of  $\varepsilon$  at these energies. At  $\varepsilon = 0.2$ , which is consistent with the LEAR data<sup>15</sup> and not in conflict with the data of Ref. 21, we obtain a good description of the experimental data on antiproton-nucleus cross sections.

Thus, by using nuclear data we can eliminate the ambi-

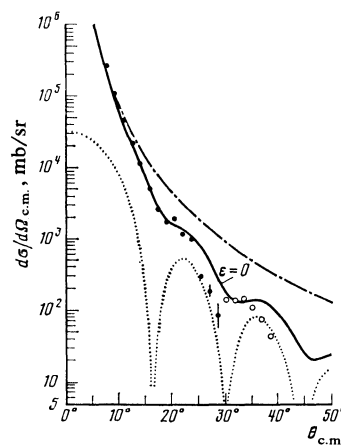


FIG. 4. Differential cross section for  $\bar{p}^{208}\text{Pb}$  elastic scattering at 46.8 MeV ( $\bullet$ ) and 47.9 MeV ( $\circ$ ). The notation is the same as for Fig. 2.

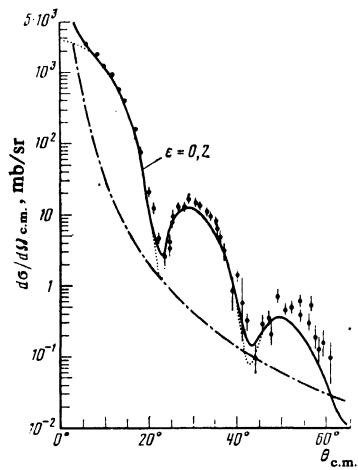


FIG. 5. Differential cross section for  $\bar{p}^{12}\text{C}$  elastic scattering at 179.7 MeV ( $\epsilon = 0.2$ ). The notation is the same as for Fig. 2.

guity that now exists in determining the value of  $\epsilon$  in the low-energy region. It is evident that by taking the antiproton-nucleus data into account we can make a choice in favor of the LEAR data.

We note that the function  $\Gamma(b)$ , which determines the amplitude for purely nuclear scattering according to Eq. (12), is virtually equal to unity within the nucleus, both in the case of antinucleon scattering, and in that of nucleon scattering (see Ref. 4). This means that for these particles the nucleus acts as an absolutely black sphere (in the central region) with a diffuse boundary. This is why the spin structure of the  $\bar{p}N$  amplitude (8), which it is very important for  $\bar{p}N$  scattering, is found to be unimportant in our calculation of the antiproton-nucleus cross sections. It should be emphasized that the effective radius of the absolutely black sphere is appreciably larger in the case of antiprotons (by a factor of 1.5 for  $^{12}\text{C}$ ) than in the case of protons because of the large tilt of the cone in the  $\bar{p}N$  amplitude.

Let us find the effective radius  $R_{\text{eff}}$  of the absolutely black sphere. We may determine it from the condition that

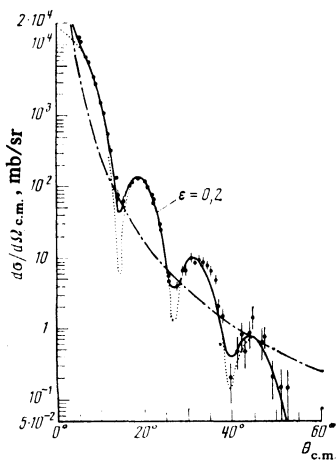


FIG. 6. Differential cross section for  $\bar{p}^{40}\text{Ca}$  elastic scattering at 179.7 MeV. The notation is the same as for Fig. 2.

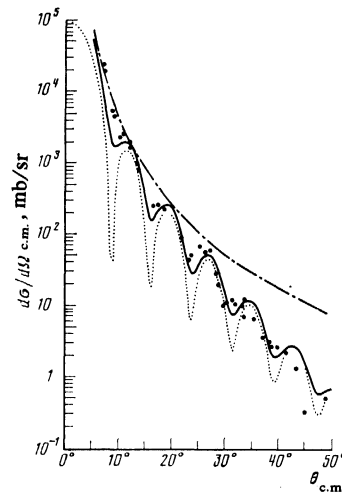


FIG. 7. Differential cross section  $\bar{p}^{208}\text{Pb}$  elastic scattering at 180.3 MeV. The notation is the same as for Fig. 2.

the cross section

$$\frac{d\sigma}{d\Omega} = \frac{k^2 R_{\text{eff}}^2}{q^2} J_1^2(qR_{\text{eff}}) \quad (19)$$

for scattering by a black sphere of radius  $R_{\text{eff}}$  should reduce to the squared modulus of the amplitude (12) when  $\theta = 0$ . We note that for Eq. (19), as well as the Glauber approximation, to be applicable it is necessary that  $kR_{\text{eff}} \gg 1$ . From Eqs. (12) and (19), we find

$$R_{\text{eff}}^2 = 2 \left| \int_0^\infty \Gamma(b) b db \right|. \quad (20)$$

For  $\bar{p}^{12}\text{C}$  scattering we obtain  $R_{\text{eff}} = 3.96$  Fm; this corresponds to the value  $r_0 = 1.73$  Fm for the coefficient  $r_0$  in the formula  $R = r_0 A^{1/3}$  and may be compared with the adopted values  $r_0 = 1.07$  Fm and  $R = 1.07 \times 12^{1/3} = 2.45$  Fm.  $R_{\text{eff}} = 3.06$  Fm for  $p^{12}\text{C}$  scattering.<sup>4</sup>

We also note that the black sphere model reproduces the  $\bar{p}^{12}\text{C}$  scattering cross section very well out to the first minimum  $q \lesssim 1$  Fm<sup>-1</sup> (see Ref. 4), despite the fact that in the case of  $\bar{p}^{12}\text{C}$  scattering the parameter  $kR_{\text{eff}} = 5.5$  is still not asymptotically large (although it is larger than the value  $kR_{\text{eff}} \approx 4$  for  $p^{12}\text{C}$  scattering). The fact that the calculated values are too large when  $q > 1$  Fm<sup>-1</sup> is due to the enhancement of the diffraction as a result of the sharp edge.

The total nuclear cross section for the  $\bar{p}^{12}\text{C}$  reaction can be expressed in terms of the function  $\Gamma(b)$  as follows:

$$\sigma_{\text{tot}} = \frac{4\pi}{k} \text{Im} F_{ii}(0) = 4\pi \int_0^\infty \text{Re} \Gamma(b) b db. \quad (21)$$

Since  $\text{Re} \Gamma(b) \gg \text{Im} \Gamma(b)$ ,  $\sigma_{\text{tot}} = 2\pi R_{\text{eff}}^2$ , where  $R_{\text{eff}}^2$  is determined by Eq. (20). Using the value obtained above for  $R_{\text{eff}}$ , we obtain  $\sigma_{\text{tot}} = 984$  mb. An integration of the elastic cross section over the angles  $\theta > 5^\circ$  [using Eq. (19)] yields  $\sigma_{\text{el}} = 464$  mb, which is in agreement with the experimental data (Ref. 1). We note that in our calculation the reaction cross section  $\sigma_r = \sigma_{\text{tot}} - \sigma_{\text{el}}$  should be  $\sigma_r = 520$  mb, which is in sharp conflict with the optical-model predictions, which yield  $\sigma_r = 620 \pm 10$  mb (see Ref. 1).

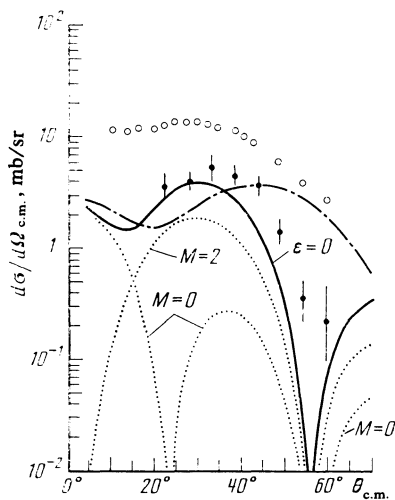


FIG. 8. Differential cross sections for  $\bar{p}^{12}\text{C}$  and  $p^{12}\text{C}$  inelastic scattering at 46.8 MeV with excitation of the  $2^+$  (4.44 MeV) level (the full and dash-dot curves, respectively). The dotted curves give the cross sections  $d\sigma_0/d\Omega$  and  $d\sigma_2/d\Omega$  for definite projections ( $M=0$  and  $M=2$ ) of the spin of the  $^{12}\text{C}^*$  ( $2^+$ ) excited nucleus onto the beam axis ( $d\sigma/d\Omega = d\sigma_0/d\Omega + 2d\sigma_2/d\Omega$ ). The experimental data are from Ref. 1.

## 6. COMPARISON WITH EXPERIMENT: INELASTIC SCATTERING

Figures 8 and 9 show the calculated  $\bar{p}^{12}\text{C}$  inelastic cross sections with excitation of the  $2^+$  (4.44 MeV) level at incident-particle energies of 46.8 and 179.7 MeV, respectively. There is satisfactory agreement with the antiproton data<sup>1,2</sup> (the full curves). In the case of the proton data (the dashed curve in Fig. 8) the calculations do not agree with experiment, as is also the case for elastic scattering (see Ref. 4).

The antiproton data are somewhat higher at  $\theta > 35^\circ$  ( $q > 0.8 \text{ Fm}^{-1}$ ) than their calculated values on Fig. 4, and there are several possible reasons for that discrepancy: a) uncertainties in the transition form factor (18); b) a decrease in the accuracy of the Glauber approximation at large scattering angles; and c) the possible collective nature of the excited  $2^+$  level together with the fact that if the level is indeed collective, the SIC approximation would not be applicable. Concerning possibility c), we note that a model in which the  $2^+$  (4.44 MeV) level is collective (rotational) would yield a larger calculated cross section for the inelastic scattering of 1-GeV protons by  $^{12}\text{C}$  (see Ref. 22) than would the shell-model calculation<sup>16</sup> and would yield a better description of the experiment. A similar case in which the experimental data in a region to the right of the maximum are higher than the values calculated using the SIC has also been observed in the cross section for excitation of the  $^{16}\text{O}^*$  ( $3^-$ , 6, 13 MeV) level by high-energy positive pions.<sup>23</sup> This discrepancy does not arise in a model in which the ( $3^-$ , 6, 13 MeV) level is assumed to be rotational, the calculation<sup>24</sup> being carried through using the Glauber theory without the SIC approximation (see Fig. 8 in Ref. 24). Similar studies of the effect of the structure of the nucleus on the intersection of antiprotons with nuclei are therefore certainly of interest.

We emphasize the fact that the amplitude for excitation

of a level is very sensitive to the surface of the nucleus.<sup>18</sup> In fact, the factor  $e^{ix} N^{(b)} = 1 - \Gamma(b)$  in Eq. (15) is zero within the nucleus and becomes unity outside the nucleus. On the other hand, the function  $\tilde{S}(b)$  damps out rapidly within the nucleus. The integral (14) is accordingly determined by the overlap region near the nuclear surface. Therefore, the function  $G_{JM}(b)$ , which determines the amplitude (14), differs from zero only in the overlap region near the nuclear surface.

We note that the calculation of the cross section for excitation of a level using the model of a black sphere with a sharp edge turns out to be very crude and yields a result that is too low by a factor of 2 or 3.

In Figs. 8 and 9, we also show the predictions for anti-proton cross sections with projections  $M$  of the spin of the excited nucleus onto the beam axis of 0 and 2:

$$\left( \frac{d\sigma}{d\Omega} = \frac{d\sigma_0}{d\Omega} + 2 \frac{d\sigma_2}{d\Omega} \right),$$

( $C_{21} = 0$  according to Eq. (16), so  $d\sigma_1/d\Omega = 0$ ). Measurements of these cross sections, which, as is evident from the figure, have very complicated angular dependences, would provide a more detailed test of the theory.

The cross section  $d\sigma_M/d\Omega$  can be easily obtained from the angular distributions of the  $\gamma$  rays emitted during the transition of the nucleus to its ground state. For  $^{16}\text{O}$ , such experiments have been made<sup>23</sup> in a beam of high-energy positive pions and protons. The angular distribution of the  $\gamma$  rays is determined by the polarization of the density matrix of the excited nucleus:

$$\rho_{MM'}(q) = F_{inel}^M(q) F_{inel}^{*M'}(q) / \sum_M |F_{inel}^M(q)|^2. \quad (22)$$

It follows from Eqs. (14)–(17) that

$$\rho_{MM'} = \rho_{-M-M'}, \quad \rho_{M-M'} = (-1)^{M'} \rho_{MM'}, \quad \rho_{-MM'} = (-1)^M \rho_{MM'}.$$

For a  $J = 2$  level, therefore, the density matrix is determined by only three independent elements:  $\rho_{00}$ ,  $\rho_{22}$ , and  $\rho_{20}$  (according to Eq. (16), the amplitude  $F_{inel}^M(q)$  differs from zero

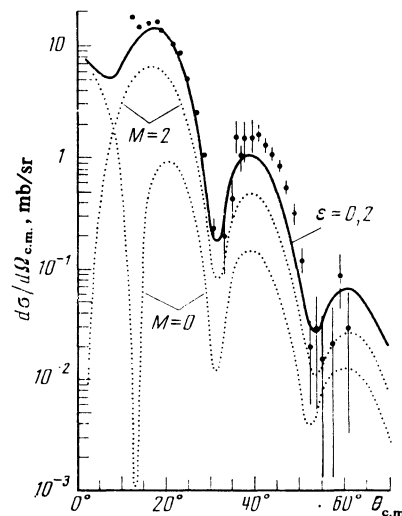


FIG. 9. Differential cross section for  $\bar{p}^{12}\text{C}$  inelastic scattering at 179.7 MeV ( $\epsilon = 0.2$ ) the excitation of the  $2^+$  (4.44 MeV) level. The notation is the same as for Fig. 8.

only for projections  $M$  that have the same parity as  $J$ ). The angular distribution of the gamma rays emitted in the transition  $J \rightarrow 0$  can be obtained from the formula

$$W(\theta_\gamma, \varphi_\gamma, q) = \sum_{MM'} \rho_{MM'}(q) Y_{JM}^{(\lambda)}(\theta_\gamma, \varphi_\gamma) Y_{JM}^{(\lambda)*}(\theta_\gamma, \varphi_\gamma), \quad (23)$$

where the  $Y_{JM}^{(\lambda)}(\theta_\gamma, \varphi_\gamma)$  are the well-known spherical vectors of the photon,  $\theta_\gamma$  is the angle between the direction of the incident beam and the momentum of the  $\gamma$  ray, and  $\varphi_\gamma$  is the angle between the scattering plane  $(\vec{p}, \vec{p}')$  and the plane defined by the momenta of the incident beam and the  $\gamma$  ray. Explicit expressions for the angular distributions of the  $\gamma$  rays emitted in the deexcitation of nuclei from  $J = 2$  and  $J = 3$  levels are given in Ref. 4.

## 7. CONCLUSION

It is evident from the calculations presented above that the theoretical curves calculated in the Glauber approximation agree well with the experimental data.<sup>1,2</sup> That the mass of data on light, medium, and heavy nuclei ( $^{12}\text{C}$ ,  $^{40}\text{Ca}$ , and  $^{208}\text{Pb}$ ) at two energies (48.6 and 180 MeV), as well as the data on inelastic scattering by  $^{12}\text{C}$ , can be described by the same parameter values (differing only for the different energies) cannot be accidental. We therefore assume that the mechanism for the interaction of antiprotons with nuclei at energies  $\gtrsim 50$  MeV may be regarded as established: that mechanism is given by the Glauber theory of multiple scattering. At such low energies, this conclusion is far from trivial and provides favorable possibilities for a subsequent joint and detailed analysis of antinucleon-nucleus and antinucleon-nucleon cross sections. We see that an analysis of antinucleon-nucleus cross sections in the Glauber approximation can be used to extract information on the  $\bar{p}N$ -amplitude parameters. For this it will be necessary to measure the antinucleon-nucleus cross sections at various incident-antinucleon energies. Detailed and precision measurements of the cross sections near their minima are especially important.

Precise measurements of the  $\bar{p}N$ -amplitude parameters (the ratio of the real to the imaginary parts of the amplitude and the inclination of the diffraction cone) in the low-energy region are also of considerable interest. Such LEAR measurements will probably be made in the very near future. More accurate measurements of the cross sections for scattering of electrons by nuclei with excitation of nuclear levels are also necessary to determine the transition form factors, which are required for calculating the antiproton-nucleus inelastic cross sections.

It is also possible to determine  $\varepsilon$  from data on the scattering of other hadrons ( $\pi$ ,  $K$ ,  $p$ ) by nuclei at energies at which the Glauber approximation is valid. To determine the ratio of the real to the imaginary parts of the elementary amplitudes for hadron scattering by nucleons, it will be necessary to have precise measurements of the hadron-nucleus cross sections at the diffraction minima.

The cross sections at the diffraction minima are very sensitive, not only to the  $\bar{p}N$ -amplitude parameters, but also to the corrections to the Glauber approximation. The very good description of the cross sections for  $^{12}\text{C}$ ,  $^{40}\text{Ca}$ , and

$^{208}\text{Pb}$  shows that at the present (already very high) level of accuracy, no clear sign of these corrections has yet been seen. The more accurate values of the elementary-amplitude parameters and the magnitudes of the antiproton-nucleus cross sections at the diffraction minima make it possible to determine the actual limits of applicability of the Glauber approach at low energies and large angles and to determine the contribution and physical nature of other less obvious and more complicated mechanisms. For a final solution of these problems, not only the empirical basis of the Glauber approach to low-energy antinucleon scattering by nuclei, but also a purely theoretical basis for that approach, starting from first principles, seem to be especially important.

It is also evident from the analysis presented above that even the first data<sup>1,2</sup> from the LEAR turned out to be very interesting and informative.

The authors thank I. S. Shapiro for his support of the work and stimulating discussions, and D. Garreta for making the new experimental data obtained by his group available to us.

<sup>1</sup>If the Coulomb scattering is neglected (this is not justified at energies of the order of 50 MeV) the cross sections for  $\varepsilon = 0$  have very deep minima, while for  $\varepsilon = -0.25$  the calculated  $\bar{p}^{12}\text{C}$  cross section accidentally agrees with the experimental data (see Ref. 4). The cross sections for  $^{40}\text{Ca}$  and  $^{208}\text{Pb}$  targets<sup>2</sup> without Coulomb scattering cannot be described by any value of  $\varepsilon$ .

<sup>1</sup>Helmut Kröger, Phys. Lett. **135B**, 266 (1984).

<sup>2</sup>D. Garreta *et al.*, Phys. Lett. **149B**, 64 (1984), Preprint CERN-EP/84-93, 114.

<sup>3</sup>R. Glauber, Third International Conference on High-Energy Physics and Nuclear Structure, Columbia University, Sept. 1969 (cited in Russian translation).

<sup>4</sup>O. D. Dalkarov and V. A. Karmanov, Phys. Lett. **174B**, 1 (1984); Pis'ma Zh. Eksp. Teor. Fiz. **39**, 288 (1984) [JETP Lett. **39**, 345 (1984)]; Pis'ma Zh. Eksp. Teor. Fiz. **41**, 47 (1985) [JETP Lett. **41**, 58 (1985)]; Preprint FIAN No. 77 (1984); No. 55 (1985).

<sup>5</sup>J. A. Niskanen and A. M. Green, Nucl. Phys. **A404**, 495 (1983); T. Suzuki, Preprint HUPD-8506, March 1985.

<sup>6</sup>C. J. Batty, Phys. Lett. **142B**, 241 (1984); K.-I. Kubo, H. Toki, and M. Igarashi, Nucl. Phys. **A435**, 708 (1985).

<sup>7</sup> $\bar{N}N$  and  $\bar{N}D$  Interactions—a Compilation, LBL-58 (1972).

<sup>8</sup>A. K. Kerman, M. McManus, and R. M. Thaler, Ann. Phys. **8**, 551 (1959).

<sup>9</sup>O. D. Dalkarov and F. Myhrer, Nuovo Cimento **40A**, 152 (1977).

<sup>10</sup>I. S. Shapiro, Phys. Reports **35**, 129 (1978).

<sup>11</sup>O. D. Dalkarov, V. M. Kolybasov, and V. G. Ksenzov, Nucl. Phys. **A397**, 498 (1983).

<sup>12</sup>L. A. Kondratyuk, M. Zh. Shmatikov, and R. Bidzarri, Yad. Fiz. **33**, 795 (1981) [Sov. J. Nucl. Phys. **33**, 413 (1981)].

<sup>13</sup>G. D. Alkhozov, S. L. Belostotsky, and A. A. Vorobyov, Phys. Rep. **42**, 89 (1978).

<sup>14</sup>R. D. Tripp In: Proceedings of the 5-th European Symposium on Nucleon-Antinucleon Interactions, Bressanone, Italy, 23-28 June, 1980, p. 519.

<sup>15</sup>R. Klapisch, Nucl. Phys. **A434**, 222 (1985).

<sup>16</sup>Robert H. Bassel and Colin Wilkins, Phys. Rev. **174**, 1179 (1968).

<sup>17</sup>R. Hofstadter, Ann. Rev. Nucl. Sci. **7**, 231 (1957).

<sup>18</sup>V. V. Balashov, Proc. 8th Summer School of the Leningrad Institute of Nuclear Physics, Leningrad, 1973, part II, p. 255; V. N. Mileev and T. V. Mischenko, Phys. Lett. **47B**, 197 (1973); L. A. Kondratyuk and Yu. A. Simonov, Pis'ma v Zh. Eksp. Teor. Fiz. **17**, 619 (1973) [JETP Lett. **17**, 435 (1973)].

<sup>19</sup>M. Bouten and P. van Leuven, Ann. Phys. **43**, 421 (1967).

<sup>20</sup>M. Cresti, L. Peruzzo, and G. Sartori, Phys. Lett. **132B**, 209 (1983).

<sup>21</sup>V. Ashford, M. E. Sainio, M. Sakitt, *et al.*, Phys. Rev. Lett. **54**, 518 (1985).

<sup>22</sup>A. N. Antonov and E. V. Inopin, Yad. Fiz. **16**, 74 (1972) [Sov. J. Nucl.

Phys. **16**, 38 (1972)].

<sup>23</sup>I. V. Kirpichnikov, V. A. Kuznetsov, I. I. Levintov, and A. S. Starostin, *Yad. Fiz.* **40**, 1377 (1984) [*Sov. J. Nucl. Phys.* **40**, 1377 (1984)]; *Yad. Fiz.* **41**, 21 (1985) [*Sov. J. Nucl. Phys.* **41**, 13 (1985)]; ITEP (Institute of Theoretical and Experimental Physics) Preprints: 96 (1979), 119

(1981), 94 (1984), 95 (1984), and 96 (1984).

<sup>24</sup>V. A. Karmanov, *Yad. Fiz.* **35**, 848 (1982) [*Sov. J. Nucl. Phys.* **35**, 492 (1982)]; H. Iwasaki *et al.*, *Phys. Lett.* **103B**, 247 (1981).

Translated by E. Brunner